Supporting Information

Polypeptide-Based Gold Nanoshells for Photothermal Therapy

Kristine M. Mayle,[1] Kathryn R. Dern,[1] Vincent K. Wong,[1] Shijun Sung,[2] Ke Ding,[1] April R.

Rodriguez,[1] Zachary Taylor,[1,4] Z. Hong Zhou,[1,3,5] Warren S. Grundfest,[1,2,4] Timothy J. Deming,[1]

and Daniel T. Kamei[1,*]

1 Department of Bioengineering, University of California, Los Angeles, CA 90095
2 Department of Electrical Engineering, University of California, Los Angeles, CA 90095
3 Department of Microbiology, Immunology & Molecular Genetics, University of California, Los Angeles, CA 90095
4 Department of Surgery, University of California, Los Angeles, CA 90095
5 California NanoSystems Institute, University of California, Los Angeles, CA 90095

*Corresponding Author: Prof. Daniel T. Kamei, kamei@seas.ucla.edu

Cytotoxicity of K$_{60}$L$_{20}$ Vesicles and Gold Nanoshells

Use of the positively charged K$_{60}$L$_{20}$ vesicles has been limited due to the high toxicity at concentrations relevant for chemotherapeutic approaches. After coating the vesicles with a thin layer of gold, the cytotoxicity of the gold nanoshells was compared with the uncoated K$_{60}$L$_{20}$ vesicles. Specifically, PC3 cells were seeded onto 96 well plates at a density of 88,000 cells cm^{-2}. Various concentrations of gold nanoshells in blank RPMI media (no fetal bovine serum, penicillin, and streptomycin) were incubated with triplicate wells of PC3 cells for 5 h. After the 5 h incubation period, the medium was aspirated and fresh medium containing the 20% MTS reagent solution (MTS cell proliferation assay; CellTiter 96® AQ$_{ueous}$ Non-Radioactive Cell Proliferation Assay) was added to the cells. The cells were then incubated in a humidified CO$_2$ incubator at 37°C for 1 h, and the absorbance was measured at 490 nm. The observed toxicity was significantly reduced after coating the K$_{60}$L$_{20}$ vesicles with gold **(Figure S1)**. We hypothesized that this is due to the gold disguising the abundance of the lysines on the vesicle surfaces, preventing harmful interactions with the net negatively charged cell membranes and reducing the overall toxicity of the carrier. To explain the increase in relative survival, as well as relative survival points above 1, we rationalized that at high gold nanoshell concentrations there is a greater absorption of light by the gold nanoshells at the wavelength of the MTS assay (490 nm with 700 nm reference). The reduction in the relative survival at the highest nanoparticle concentration was reasoned to be due to the toxicity caused by such a high concentration. For the decrease in relative survival for the uncoated K$_{60}$L$_{20}$ vesicles, we rationalized that it was due to the positively charged amine groups on the uncoated K$_{60}$L$_{20}$ surface interacting with the negatively charged cell membranes, causing cytotoxicity.
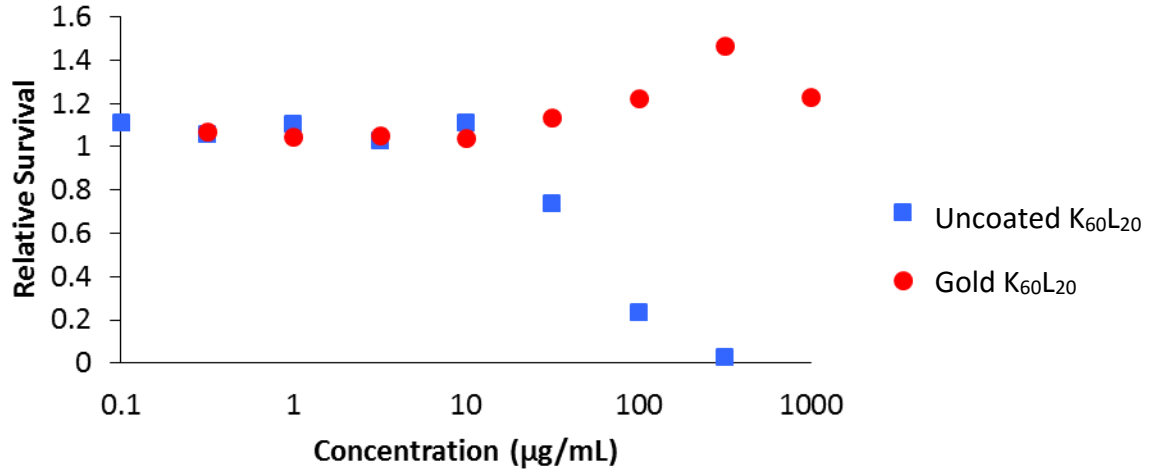
Figure S1. Cytotoxicity for uncoated $K_{60}L_{20}$ vesicles (blue) and $K_{60}L_{20}$ gold nanoshells (red).

Mathematical Model for Heat Transfer in Suspensions Containing Gold Nanoshells

A model for the heating of the well due to laser irradiation of the gold nanoshells, as well as the subsequent heat transfer, was developed by using the differential form of the conservation of energy equation. In this model, it is assumed that only the gold nanoshells within the path of the laser generate heat, and the heat is then conducted to the region outside of the path of the laser. For this approach, two regions were defined. The region in the path of the laser (the inner cylinder) was modeled using **Eq. S1**, while the region outside of this path (the cylindrical annulus) was modeled with **Eq. S2**.

$$\rho C_p \frac{\partial T}{\partial t} = k \nabla^2 T + Q_{laser} \qquad (S1)$$

$$\rho C_p \frac{\partial T}{\partial t} = k \nabla^2 T \qquad (S2)$$

The $\rho C_p \frac{\partial T}{\partial t}$ term on the left hand side is related to the change in energy with respect to time of a differential volume of solution. The $k\nabla^2 T$ term on the right-hand side is associated with heat conduction, and **Eq. S1** has an additional term, Q_{laser}, which is associated with the heat generated due to plasmonic heating of the gold nanoshells due to laser irradiation. In these equations, T is temperature (K), t is time (s), k is the thermal conductivity (W m^{-1} K^{-1}), ρ is the density (kg m^{-3}), and C_p is the heat capacity (J kg^{-1} K^{-1}). The parameters used in the model are shown in **Table S1**.

Heat Generation by Gold Nanoshells (Q_{laser})

Q_{laser} (W m^{-3}) is the heat generated by the gold nanoshells, which has been described previously by the following equation, which assumes all energy absorbed will be converted to heat:[1]

$$Q_{laser} = (\sigma_{abs} C_{GKL})I \tag{S3}$$

where σ_{abs} is the absorption coefficient (m^2 mol^{-1}), C_{GKL} is the concentration of gold nanoshells (mol m^{-3}), and I is the laser power density (W m^{-2}), where the laser power (0.2 W based on the purchased laser) was assumed to be equally distributed to the gold nanoshells within the irradiated region of the well. Furthermore, if one assumes all energy is absorbed by the gold nanoshells (neglecting the scattering of the light), the Beer-Lambert law can be used to replace the $\sigma_{abs}C_{GKL}$ term on the right hand side of **Eq. S3** with A/g, where A is the absorbance of the gold nanoshells at 808 nm, and g is the path length of the cuvette used in the UV-visible spectrophotometer (0.01 m):

$$Q_{laser} = \frac{A}{g} I \qquad \text{(S4)}$$

To estimate the absorbance of the gold nanoshells, A, the Mie Theory was applied to determine the fraction of absorption cross-sectional area compared to the total extinction cross-sectional area, where extinction is the sum of the scattering and absorption of light by the gold nanoshells.[2–4] Based on the core diameter, shell thickness, and refractive indices of water and gold, the majority of light is scattered by the gold nanoshells, where approximately 10% of the total light energy is absorbed. Therefore to calculate A, the extinction at 808 nm was measured using a UV-Vis spectrophotometer, and then it was multiplied by 0.10.

Furthermore, the laser power density, I, was expected to be attenuated along the z-direction as light was scattered and absorbed by the gold nanoshells. To predict the power density as a function of depth, the Beer-Lambert Law was used:

$$I = I_0 * 10^{-(\varepsilon C_{GKL})z} \qquad \text{(S5)}$$

where I_0 is the incident laser power density, ε is the extinction coefficient ($m^2\ mol^{-1}$), and z is the vertical depth in the well. Here the extinction coefficient is used, since laser attenuation is due to the sum of the scattering and absorption of light, also known as extinction. The Beer-Lambert Law was used to replace the εC_{GKL} term with OD/g, where OD is the extinction (i.e., optical density) as measured by the UV spectrophotometer.

Boundary Conditions

In order to solve the above equations, the following boundary conditions in the radial and z-directions, as well as an initial condition, were applied. For the first boundary condition in the

radial direction, we set the heat flux due to conduction to zero at the center (r = 0) due to axisymmetry:

$$-k\frac{dT}{dr}\bigg|_{r=0} = 0 \tag{S6}$$

where k is the thermal conductivity of a GKL suspension, which is slightly higher than the thermal conductivity of water alone. The high concentration of GKL increases the conductivity of the suspension. In fact, this same assumption has been made in similar energy conservation mathematical models for capturing the photothermal therapy effect of gold nanorods.[5] The second boundary condition in the radial direction describes the heat flux to the outer region (r = R1), which is equal to the heat flux from the irradiated region **(Eq. S7).**

$$-k\frac{dT}{dr}\bigg|_{r=R1^-} = -k\frac{dT}{dr}\bigg|_{r=R1^+} \tag{S7}$$

where R1 is the radius of the irradiated region, R1⁻ is the radial position just left of r = R1 in the aqueous suspension of the irradiated region, and R1⁺ is the radial position just right of r = R1 in the aqueous suspension in the outer region.

The third boundary condition in the radial coordinate assumes equilibrium of temperature at the boundary of the irradiated region (r = R1) **(Eq. S8).**

$$T\big|_{r=R1^-} = T\big|_{r=R1^+} \tag{S8}$$

The fourth boundary condition in the radial coordinate states that the heat flux in the suspension to the wall due to conduction (r = R2) is equal to the flux away through the wall **(Eq. S9).**

$$-k\frac{dT}{dr}\bigg|_{r=R2^-} = -k_{wall}\frac{dT_{wall}}{dr}\bigg|_{r=R2^+} \tag{S9}$$

where k_{wall} is the thermal conductivity of the polystyrene wall,[6] T_{wall} is the temperature of the wall, R2 is the radius of the well, R2⁻ is the radial position just left of r = R2 in the aqueous suspension, and R2⁺ is the radial position just right of r =R2 in the wall. For this model, we assumed that the temperature gradient through the wall is linear, and therefore, **Eq. S9** can be simplified to the following:

$$-k\frac{dT}{dr}\bigg|_{r=R2^-} = U_{wall}(T_{wall,in} - T_{wall,out}) = U_{wall}(T(r = R2^-) - T_{wall,out}) \tag{S10}$$

where $U_{wall} = k_{wall}/d$, d is the thickness of the wall (measured to be 1 mm), $T_{wall,in}$ is the temperature of the inner wall that is equal to the temperature in the aqueous suspension at r=R2⁻, and $T_{wall,out}$ is the outer temperature of the wall, which was assumed to be 290 K.

The first boundary condition in the z-direction is located at the bottom of the well, and is similar to **Eq. S9**. Specifically, the heat flux in the suspension to the bottom of the well (z =0) is set equal to the heat flux through the wall:

$$k\frac{dT}{dz}\bigg|_{z=0^-} = k_{wall}\frac{dT_{wall}}{dz}\bigg|_{z=0^+} \tag{S11}$$

where z = 0⁻ is the z-coordinate just below the bottom position of the well in the solid wall, and z = 0⁺ is the z-coordinate just above the bottom of the well in the aqueous suspension. Similar to **Eq. S10**, we assumed that the temperature gradient through the wall is linear, and **Eq. S11** can be simplified to:

$$k\frac{dT}{dz}\bigg|_{z=0^-} = U_{wall}(T_{wall,in} - T_{wall,out}) = U_{wall}(T(z = 0^+) - T_{wall,out}) \tag{S12}$$

where $U_{wall} = k_{wall}/d$, d is the thickness of the wall (measured to be 1 mm), $T_{wall,in}$ is the temperature of the inner wall that is equal to the temperature in the aqueous suspension at $z=0^+$, and $T_{wall,out}$ is the outer temperature of the wall, which was assumed to be 290 K. The second boundary condition in the z-direction corresponds to the heat flux in the suspension to the water-air surface ($z = H$) being equal to the heat convected away from the surface and the heat lost due to evaporative cooling at the water-air interface:

$$-k\frac{dT}{dz}\bigg|_{z=H^-} = h_{air}\left(T_{air,s} - T_{air,b}\right) + \frac{\dot{m}H_{vap}}{S} = h_{air}\left(T(z=H^-) - T_{air,b}\right) + \frac{\dot{m}H_{vap}}{S} \qquad (S13)$$

where h_{air} is the convective heat transfer coefficient for air (which was estimated with empirical correlations[7]), $z = H^-$ indicates the position just below the water-air interface in the aqueous suspension, $T_{air,s}$ is the temperature of the air at the water-air interface (which is equal to the temperature of the aqueous suspension at that same position), $T_{air,b}$ is the bulk temperature of the air (290 K), $\dot{m}$ is the average rate of water loss to evaporation (which was estimated

experimentally using the mass of water appearing as condensate on the wall of the tube), H_{vap} is the heat of vaporization of water,[7] and S is the surface area of the well (estimated to be 32 mm^2).

The initial temperature condition for the entire aqueous suspension (t =0) was set to the initial temperature of (T_i) 290K:

$$T(r, z, t = 0) = T_i \qquad \text{(S14)}$$

For this model, we numerically solved the partial differential equations in both defined regions (inner cylinder and outer annulus) using finite difference equations and the method of lines.

Table S1. Parameters used for our mathematical model of heat transfer.

Parameter	Description	Value
ρ	Fluid density	1000 kg m^{-3}
I_0	Incident laser power density in water	3.33×10^5 W m^{-2}
C_p	Fluid heat capacity	4184 J kg^{-1} K^{-1}
OD	Extinction (i.e., Optical Density)	0.6 a.u.
k	Thermal conductivity of GKL in water	0.75 W m^{-1} K^{-1}
U_{wall}	Thermal conductivity through the wall	100 W m^{-2} K^{-1}
T_{wall}	Temperature of wall	290 K
h_{air}	Convective heat transfer coefficient of air	15 W m^{-2} K^{-1}
T_{air}	Temperature of air	290 K
$\dot{m}$	Average rate of mass loss to evaporation	3.3×10^{-8} kg s^{-1}
H_{vap}	Heat of vaporization	2.46×10^6 J kg^{-1}

References (Supporting Information)

1. Elliott A, Schwartz J, Wang J, Shetty A, Hazle J, Stafford JR. Analytical solution to heat equation with magnetic resonance experimental verification for nanoshell enhanced thermal therapy. *Lasers Surg Med*. 2008;40(9):660-665. doi:10.1002/lsm.20682.

2. Oldenburg S., Averitt R., Westcott S., Halas N. Nanoengineering of optical resonances. *Chem Phys Lett*. 1998;288:243-247. doi:10.1016/S0009-2614(98)00277-2.

3. Morton JG, Day ES, Halas NJ, West JL. Nanoshells for photothermal cancer therapy. *Methods Mol Biol*. 2010;624:101-117. doi:10.1007/978-1-60761-609-2_7.

4. Averitt RD, Westcott SL, Halas NJ. Linear optical properties of gold nanoshells. *J Opt Soc Am B*. 1999;16(10):1824. doi:10.1364/JOSAB.16.001824.

5. Huang H-C, Rege K, Heys JJ. Spatiotemporal temperature distribution and cancer cell death in response to extracellular hyperthermia induced by gold nanorods. *ACS Nano*. 2010;4(5):2892-2900. doi:10.1021/nn901884d.

6. Callister W. *Materials Science and Engineering: An Introduction*. 6th ed. Wiley; 2002.

7. Incopera F, Dewitt D, Bergman T, Lavine A. *Introduction to Heat Transfer*. 5th ed. Wiley; 2006.